CEAS Aeronautical Journal (2021) 12:509–518
https://doi.org/10.1007/s13272-021-00507-9

ORIGINAL PAPER

# Structural concept of an adaptive shock control bump spoiler

**Markus Kintscher**[1] · **Johannes Riemenschneider**[1] · **Hans-Peter Monner**[1] · **Martin Wiedemann**[1]

Received: 2 May 2019 / Revised: 2 March 2021 / Accepted: 31 March 2021 / Published online: 21 April 2021


**Abstract**
Drag reduction technologies in aircraft design are the key enabler for reducing emissions and for sustainable growth of commercial aviation. Laminar wing technologies promise a significant benefit by drag reduction and are, therefore, under investigation in various European projects. However, of the established moveable concepts and high-lift systems thus far most do not cope with the requirements for natural laminar flow wings. To this aim, new leading edge high-lift systems have been the focus of research activities in the last 5 years. Such leading edge devices investigated in projects include a laminar flow-compatible Kruger flap (Schlipf (2011) Insect shielding Krüger—structural design for a laminar flow wing. In: DGLR Congress 2011, Bremen, pp 55–60) and the Droop Nose concept (Kintscher et al. Ground testof an enhanced adaptive droop nose device. In: European Congress on Computational Methods in Applied Sciences and Engineering, ECCOMAS 2016. ECCOMAS2016—VII European Congress on Computational Methods in Applied Sciences and Engineering, 5–10 June 2016, Crete Island, Greece; Kintscher et al. Low speed wind tunnel test of a morphing leading edge. In: AIDAA—Italian Association of Aeronautics and Astronautics XXII Conference, 09–12 Sept. 2013. Neapel, Italien) and these can be considered as alternatives to the conventional slat. Hybrid laminar flow concepts are also under investigation at several research institutes in Europe (Fischer. Stepless and sustainable research for the aircraft of tomorrow—from AFloNext to Clean Sky 2. In: 1st AFloNext Workshop Key Note Lecture No. 1, Delft, The Netherlands, 10 Sept 2015). Another challenge associated with laminar wings aside from the development of leading edge movables is the need to address the control of aerodynamic shocks and buffeting as laminar wings are sensitive to high flow speeds. Here, one possible method of decreasing the wave drag caused by the aerodynamic shock is through the use of shock control bumps (SCBs). The objective of SCBs is the conversion of a single strong shock into several smaller and weaker λ-shocks resulting in a drag benefit when deployed correctly. A particular desirable characteristic of SCBs is that they should be adaptable in position and height as the shock position changes with varying conditions such as speed, altitude, and angle of attack during the flight. However, as a fixed case, SCBs can also help to control laminar buffeting by fixing the shock into given positions at the SCBs location. In this paper, a structural concept for an adaptive shock control bump spoiler is presented. Based on a concept of a fixed bump SCB spoiler, a design for an adaptive spoiler with two conventional actuators is presented. Design drivers and interdependencies of important design parameters are discussed. The presented design is simple and aims for a high TRL without adding much complexity to the spoiler. It is robust and able to form a bump with a height of 0.6% chord length which position can be adapted in a range of 10% chord. This paper is a follow-up of a previous publication (Kintscher and Monner, SAE Tech Paper 10.4271/2017-01-2164, 2017) with extending the focus by a validation of computational results by experimental tests.

**Keywords** Morphing · Adaptive structures · Shock control bump

## 1 Introduction

For drag reduction, laminar flow and hybrid laminar flow technologies are currently under investigation in many European projects. In these projects great attention has been given to laminar compatible leading edge devices in the past 5 years. In the German Aerospace Center, the Kruger Slat and Smart Droop Nose Devices have especially been

✉ Markus Kintscher
markus.kintscher@dlr.de

[1] Deutsches Zentrum Für Luft- und Raumfahrt, Institut für Faserverbundleichtbau und Adaptronik, Lilienthalplatz 7, 38108 Braunschweig, Germany

investigated as a replacement for the conventional slat. On the leading edge, a high-lift device with a continuous upper skin panel is mandatory as an enabler for laminar flow. The Kruger device is one promising candidate due to the fact that a shielding functionality can be integrated to avoid contamination of the leading edge surface by insects. The smart droop nose has the disadvantage of decreased aerodynamic performance compared to a slat or Kruger device but offers a significant potential for noise reduction with moderate aerodynamic performance. However, the trailing edge devices play a role in drag reduction as well. With the advanced dropped hinge flap, Airbus introduced multifunctional moveable devices in the A350 design to realize opportunities like active load control, variable camber for cruise performance and differential flap setting for optimization of load distribution. With the advanced dropped hinge flap, the high-lift aerodynamic efficiency is optimized through the control of the spoiler–flap gap. Subsequently, the adaptive shock control bump spoiler is the next step towards high performance laminar wings [1–6].

The wave drag reduction potential of shock control bumps has been demonstrated widely [6–8] (Fig. 1).

The idea behind using shock control bumps is that they can control the shock to reduce wave drag and/or extend the flight envelope which often is limited by buffeting. The effect is based on a deceleration of the flow in a limited region of approximately 20–25% of the chord length [9]. On the upstream side of the bump, isentropic compression waves are created, leading to a series of shocks and to a decreasing Mach number in front of the main shock. This significantly decreases the shock in case of a well-shaped and positioned bump.

In [9], Sommerer et al. presented results of the numerical optimization of adaptive transonic airfoils with variable camber and shock bump control. The results give an encouraging potential for the application of SCBs on a transonic airfoil. For a specified off-design condition, Sommerer optimized bump shapes and investigated the influence of various geometric bump representations. It is found that the detailed shape of the bump is of minor importance; while bump position, i.e., the location of the bump crest, and height play a major role for the bump effectiveness. Therefore, the structural design of a shock control bump should be able to adapt the bump height and position to the off-design and flow conditions to get the maximum drag reduction. Based on these findings, a generic geometry is used for the design of the position-adaptable SCB spoiler concept with consideration of the guidelines and recommendations for the SCB design given in Table 1 and Fig. 2.

A prerequisite for the SCB spoiler is laminarity since the shock is located at the trailing edge of the main wing at about 60–70% chord in the region where the spoilers are located for only this characteristic pressure distribution.

In [10], the envisaged bump height is given as approximately 0.1–0.5% of the chord length and the bump length is estimated as 15–20% chord. It is important to understand that for a large part of the wing span, this relates to the full spoiler chord length. The variation of the shock position and, therefore, of the optimal bump crest position during flight due to varying pressure distribution is assumed to be approximately 10% chord length. This corresponds to approximately half of the complete spoiler chord length. Investigations of Sommerer [9] show that there is a possibility to limit the shock chord length variation and to decrease the necessary bump height by a flap with variable camber functionality. However, in this study, the intention is to identify the extremal configurations and the corresponding design drivers and consequences for the design. The effect of a variable camber flap is not considered.

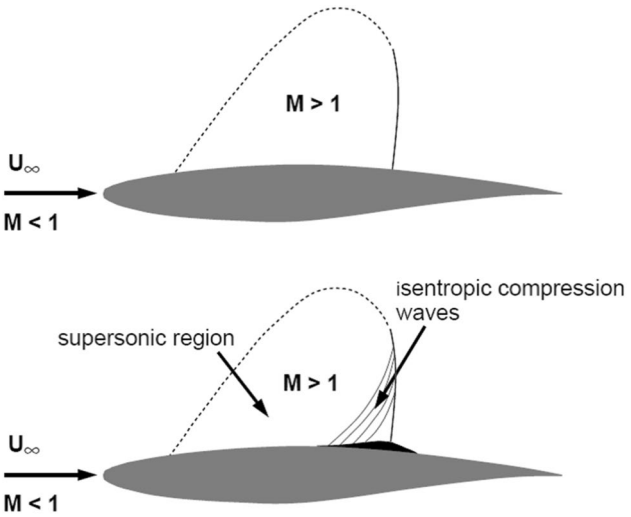


**Fig. 1** Aerodynamic concept of shock control bumps from [9]

**Table 1** Geometric definitions for the investigation of a position variable SCB

| | |
|---|---|
| $x_c/c$ | 0.60–0.70 |
| $l_b/c$ | 0.15–0.30 |
| $h_b/c$ | 0.001–0.005 |

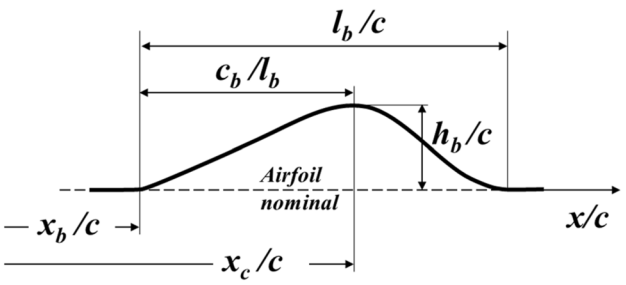


**Fig. 2** SCB geometry definition

While many research groups have focused on the aerodynamic design of SCBs and the corresponding drag reduction potential, only limited information is available regarding the structural design concepts and realization of such devices. The challenge in the structural design of an adaptive shock control bump device is the combination of structural stiffness, actuation and available space. While the structure itself has to be flexible enough to provide the desired shape change by actuation, the actuation forces must be as low as possible since high actuation forces require large actuators. This is undesired due to the resulting weight penalty and the small design space available at high aspect ratio wings, especially at the outboard region of the wing.

Bein et al. [11] presented a concept for actuation of an adaptive SCB in 1998 using a tube spring. The concept is based on the tube spring actuator driven either by pressure or shape memory alloy (SMA). Both methods of actuation have been verified by experimental investigations. However, the integration into the spoiler body and a design of a flexible spoiler skin is not presented. Another actuator concept based on SMA was proposed by Campanile et al. in [12] with the "fish-mouth" actuator. It is developed at the German Aerospace Center (DLR) in the framework of the Adaptive Wing project (ADIF). It is a compact hybrid actuator based on the interaction of a shape memory material and a composite flexible mechanism. 86 actuators were integrated into the trailing edge skin of a wind tunnel model with a glass fiber reinforced skin. With a maximum actuator stroke of two millimeters only small displacements can be induced with this concept. Wadehn et al. [13] used this actuator concept for a combined aerodynamic and structural design process including a control concept. The proposed combined design and control concept was tested in a model of an adaptive spoiler which was manufactured as a sandwich structure with integrated Moonie kinematics actuated by shape memory actuators. The concept showed desirable geometric accuracy and robustness against external disturbances whilst the actuator forces are only moderate. An integrated design concept is presented by the author in [14]. A spoiler body with pressurized cells is designed for an adaptive SCB (Fig. 3).

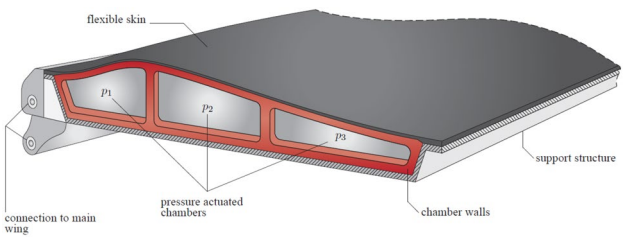


**Fig. 3** Structural concept with pressurized cells for realization of a shock control bump spoiler by Sousa from [14]

The cells are integrated into the spoiler body and can provide different SCB shapes depending on the pressurization of the cells. The design is based on analytical formulations for a fast optimization process. A design process for preliminary design of the presented concept is proposed considering the generation of target shapes with consideration of mechanical boundary conditions.

A concept based on conventional technologies is presented by Kirn and Machunze [10, 11, 15]. The proposed concept of a position fixed SCB with variable height is based on a pre-shaping of the spoiler body. The spoiler skin and body is manufactured in a shape which is not equal to the clean cruise shape of the wing. Instead, the spoiler is pre-shaped as depicted in Fig. 3 (Fig. 4).

The contact to the flap body and the conventional spoiler actuator can then be used to adjust the shape of the upper spoiler surface to a needed bump height or to the clean cruise shape. The bump position in chord is determined by the flexible region in the spoiler structure and is fixed. The idea is based on the assumption that the shock position at the wings trailing edge can be controlled by a variable camber flap.

## 2 Structural concept

The position-adaptive SCB spoiler concept is based on the concept for a fixed SCB from Kirn and Machunze proposed [10, 11]. A second actuator is applied to the concept enabling the control of a second bump position. The basic idea of a pre-shaped spoiler body is kept but extended to a maximum backward and a maximum forward bump position. In between these positions, an adaptive SCB can be actuated and positioned depending on the flow conditions. A second hinge position at the spoilers' trailing edge is given by the end of a stiffened part of the spoiler body. The bump position can then be controlled in the region between the chord position of the first and the second hinge depending on the stiffness tailoring and the actuator displacements.

The maximum chord variability of the SCB is then defined by the parameters:

- Actuator force limits

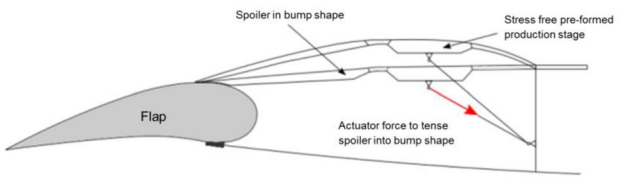


**Fig. 4** Structural concept for a shock control bump spoiler by pre-shaping by Kirn and Machunze from [10]

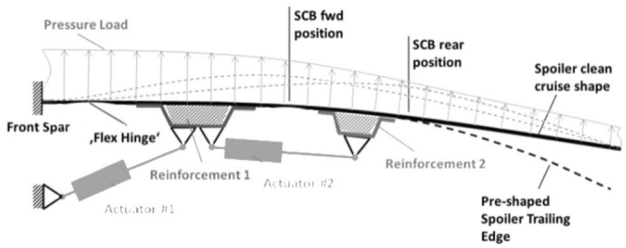


**Fig. 5** Sketch of the adaptive SCB-Spoiler (reference) concept with main contributing elements

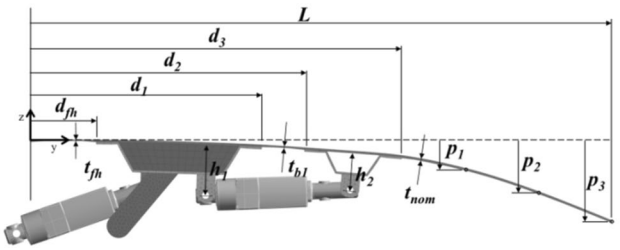


**Fig. 6** Sideview of the FE model of the adaptive SCB-Spoiler (reference configuration) concept with main design parameters

- Pre-shaping
- Local thickness
- Aerodynamic loading
- Required contact force to flap

A brief sketch of the concept with the main characterizing elements is given in Fig. 5.

Since the design proposal for the position-adaptive SCB focuses especially on the shock control for wings with natural laminar flow, the 'flexible hinge' concept for the attachment of the spoiler to the wing box as presented by Kirn is adopted. However, since the flex-hinge technology is independent of the SCB technology, it is used here as a design constraint only and not considered in detail by the author. For a sealing of the flap gap in cruise position, the spoiler needs to be in contact with the flap body. This requires a line contact of the spoiler trailing edge with the flap with a certain contact force.

## 2.1 2D concept and design load cases

To have a fast computational model for the structural analysis and optimization of the concept, a 2D extruded FE model with a span of 200 mm is created. For the adaptation of the bump position, the model is parametrized with the following main design parameters:

1. End position of the first rigid part ($d_1$)
2. Start and end position of the second rigid part ($d_2$, $d_3$)
3. Local thicknesses ($t_n$)
4. Pre-shaping of the trailing edge ($p_1$–$p_3$)

For the definition of the pre-shaping a spline with three control points $p_1$–$p_3$ at the spoiler trailing edge is used (Fig. 6).

The objective of the 2D model is the investigation of achievable maximum forward and maximum backward bump positions and the identification of design drivers and limitations of the concept. Resulting parameters for a more detailed analysis and optimization in 3D are maximum forward/backward position $b_1/b_2$ with SCB heights $b_{h1}/b_{h2}$, and actuator forces $f_1$ and $f_2$.

For the best design solution, finally, the attachment points of the second actuator have to be optimized for a balanced design which combines robustness against (varying) aerodynamic loads and effective actuation with consideration of other constraints such as the contact force of the spoiler trailing edge to the flap body or design space for example.

Besides the characteristic design parameters, the adaptivity of the concept depends on the load cases considered in the design. Since the concept assumes a pre-shaping of the spoiler body which deviates from the optimal profile shape for clean cruise flight, this is one of the most important design load cases. Here, especially waviness and contour accuracy of the retracted SCB have to be checked carefully. For the overall deviation from the nominal profile, a limit of $\pm 0.5$ mm is assumed. The surface waviness is assumed as a local deformation to the ideal flight shape and, hence, will be assessed as an increment from the nominal wing surface profile as deflected in flight.

The maximum allowed wave amplitude is assumed with $b = 3$ mm. For the ratio of amplitude to half-wave length, a value of $b/a \leq 0.005$ is used. Since waviness in the chord wise direction is significantly more critical than in span direction, the waviness is considered for this case only. Finally, the aerodynamic loading is considered as a combination of the pressures on the lower and upper side of the spoiler. As a worst case scenario, a defect sealing on the lower side is assumed. A uniform pressure of 4000 Pa is applied to the spoiler surface. To analyze the sensitivity of the adaptive SCB design the aerodynamic load is varied by about $\pm 10\%$ to check the robustness of the pre-shaping. For the assessment of the actuator forces of the first actuator, the 'Airbrake' load case is considered with a deployed spoiler of about 40° and a resulting estimated uniform pressure of 5000 Pa on the upper spoiler surface. Since conventional CFRP material is assumed for the spoiler upper cover a strain limit of 5000 μstrains is used for the design.

**Table 2** Reference configuration of the adaptive SCB spoiler

| | |
|---|---|
| Wing section chord ($w_c$) | 3330 mm |
| Skin spline length ($L_s$) | 785 mm/800 mm/24%c |
| Spoiler length ($L$) | 785 mm |
| Spoiler model span ($s$) | 200 mm |
| Spoiler TE skin thickness ($t_{nom}$) | 3 mm |
| Spoiler skin layer orientation | [45, 0, −45, 0 s] in chord |
| TE pre-shape droop ($p_3$) | 95 mm |
| Reinforcement 1 ($d_1$) | 312 mm |
| Reinforcement 2 ($d_2/d_3$) | 370 mm/500 mm |
| Max. backward SCB Crest pos./height | 500 mm/9 mm (contact force ~0 N) |
| Max. forward SCB crest pos./height | 345 mm/12.5 mm (limit strain 0.25%) |
| Max. backward actuator stroke 1/2 | 1.8 mm/0 mm |
| Max. forward actuator stroke 1/2 | 4 mm/−4 mm |

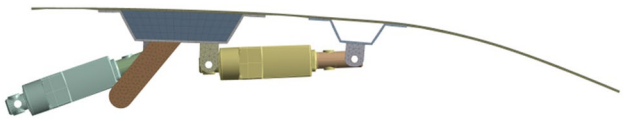

**Fig. 7** Reference configuration for the position-adaptive shock control bump

## 2.2 Reference design

A reference design is created as a starting point for the identification of design drivers of the here-presented concept of a position-adaptive SCB. The main geometrical data, the reference maximum backward bump crest position as well as the maximum forward bump crest position with corresponding actuator displacements are given in Table 2.

The maximum backward and forward positions of the bump are identified by adjustment of the actuator stroke $u_1$ and $u_2$ of the first and second actuator while considering limitations and constraints mentioned before. Steps for the setup of the reference configuration are:

1. Definition of the max. trailing edge droop ($p_3$)
2. Identification of parameters pn for optimal pre-shaping to attain the clean cruise shape within the limit of ±0.5 mm
3. Identification of $u_1$ and $u_2$ for max. backward position
4. Identification of $u_1$ and $u_2$ for max. forward position.

It is assumed that a constant gradient of the rising and falling slope of the SCB is desired due to aerodynamic purposes. Besides this the adjustment to the clean shape with an accuracy of about ±0.5 mm has highest priority.

The resulting maximum forward and backward position and SCB bump shape of the reference configuration is given in Fig. 7. The adjustment of the clean cruise shape is unproblematic and can be achieved using the control points $p_1$–$p_3$ as presented in Fig. 6. However, the variation of the vertical position of the spline control points can result in small waviness (Fig. 8).

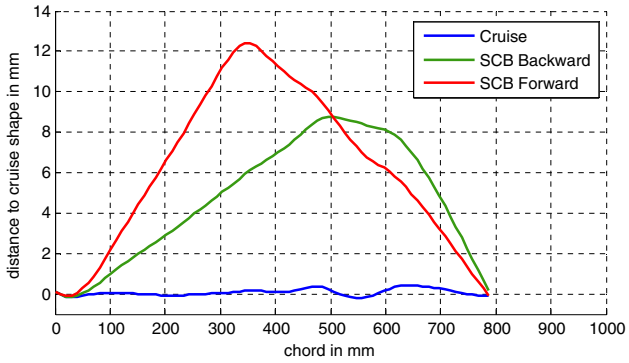


**Fig. 8** Maximum forward (345 mm) and backward (500 mm) bump crest position of the reference configuration

Consequently, any deviations from the cruise target shape will naturally affect the forward and backward SCB shape. This can be avoided by a smoothing function in the spline generation.

## 2.3 Identification of design drivers

The main design parameters for the structural design of a shock control bump are the maximum forward and backward position as well as the corresponding heights of the bump given by the aerodynamic analysis. Therefore, it is important to identify the design drivers.

For the forward position, the first actuator defines the ascending slope of the bump and the bump height; whilst, the second actuator controls the descending slope topology and the contact force to the flap body. The maximum forward position is positioned in between the positions of the reinforcement structures $d_1$ and $d_2$. Naturally, this could be adjusted by

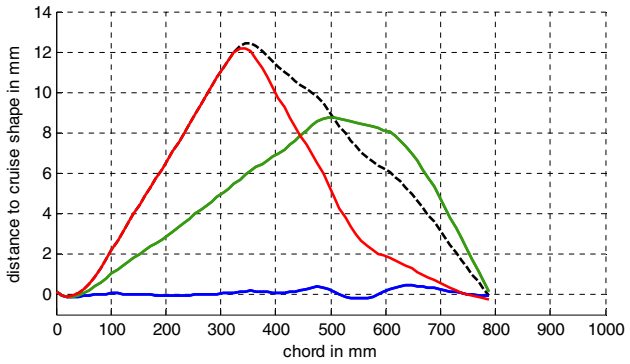


**Fig. 9** Control of the descending slope gradient using the second actuator (dashed, black—reference configuration as in Fig. 7)

modification of the skin thickness by ply tapering between the reinforcements. In this context, the SCB height is variable and the maximum height is only limited by the maximum allowable strain in the skin material and/or the actuation force limit or size limit. The maximum SCB height is directly dependent on the skin material and the skin thickness in between the positions $d_1$ and $d_2$. The descending slope can be realized with constant gradient or bi-linear gradient using the spoilers' trailing edge flexibility as depicted in Fig. 9. For the rearward position of the bump, the first actuator defines the ascending slope of the bump; whilst the second actuator defines the rearward chord position, height and contact pressure to the flap body. The maximum backward position of the shock control bump is defined by the trailing edge reinforcements end position ($d_3$).

At this position the out-of-plane bending stiffness is changing (assuming a constant trailing edge skin thickness) and most of the deformation occurs here. A design driver for the maximum backward position and maximum SCB height can be the required contact force of the spoiler trailing edge to the flap body. To guarantee a sealing function to seal the flap shroud, the contact force should not be less than zero to avoid any flow from the lower side to the upper side of the profile. When deploying the maximum backward position by actuation (just the first actuator deploys, the second actuator is locked), the spoiler is lifted and the contact force of the spoiler trailing edge to the flap body is decreasing. However, the contact force can be controlled by the length of the free spoiler trailing edge, the skin thickness and the maximum pre-shaping of the spoiler trailing edge ($p_3$). The descending slope of the maximum backward bump is defined by the pre-shaping.

For the study of variable SCB positions, the position and geometry of the first and second rigid part/reinforcements are varied. To fix the forward bump crest position, the second stiffener is extended (geometric parameters $d_1$, $d_2$ and $d_3$). For the objective for the SCB bump crest variation, it is assumed that the optimal bump crest position can vary in a range of about 10% chord length. For the selected 2D section, this means a range of the bump crest position of about 300 mm. For the attachment of the primary actuator for spoiler deployment for the airbrake functionality, the maximum forward position of the bump is assumed to be realized at about 300 mm of the spoiler length. For the maximum backward position, about 600 mm of the spoiler length is envisaged.

The extension of the trailing edge reinforcement in direction of the spoilers' trailing edge ($d_3$) leads to a smaller free unsupported length of the spoiler trailing edge and with this to a higher contact force of the spoiler trailing edge to the flap upper cover. In Fig. 10, the effect of an extension from 500 to 590 mm end position of the trailing edge reinforcement is presented. With identical actuation parameters (see Table 2), the bump crest position is shifted by 100 mm to the trailing edge resulting in a slightly increased bump height.

Due to the increased contact force to the flap, the bump height can be further increased by a larger actuator stroke of the first actuator so that a maximum bump height of about 20.7 mm (~0.6% chord) can be achieved. The summary of the characteristic data for maximum backward position configuration is given in Table 3.

Since the only limitation of the maximum forward bump height in this configuration is the strain in the skin structure, the bump height can be increased without any problems to be in similar magnitude as the backward SCB height (see Fig. 12).

The maximum forward position of the shock control bump is limited by the design space needed for a proper interface design of the actuator attachment. For a more forward position the size of the reinforcement at the spoilers' leading edge must be reduced. Since high loads are expected from the airbrake functionality, the interface design must consider the load transfer of the resulting aerodynamic loads from the spoiler into the rear spar/box structure for which a larger bracket design is beneficial.

Unfortunately, the elongation of the trailing edge reinforcement leads to a reduction in stiffness in this part. To

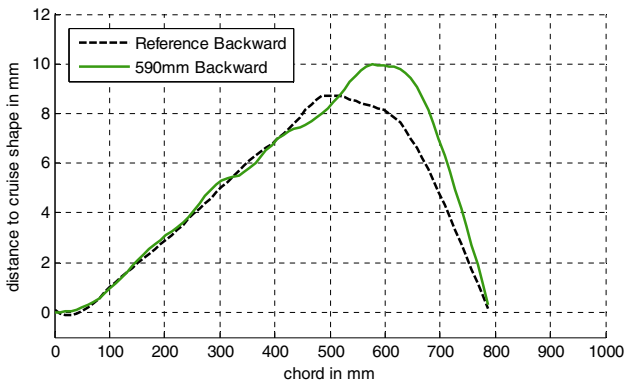


**Fig. 10** Maximum backward position SCB for d3 = 590 mm at the same actuation parameters as the reference (dashed, black—reference configuration as in Fig. 7)

**Table 3** Maximum backward configuration of the adaptive SCB Spoiler

| | |
|---|---|
| Wing section chord ($W_c$) | 3330 mm |
| Skin spline length ($L_s$) | 785 mm/800 mm/24%c |
| Spoiler length ($L$) | 785 mm |
| Spoiler model span ($s$) | 200 mm |
| Spoiler TE skin thickness ($t_{nom}$) | 3 mm |
| Spoiler skin layer orientation | [45, 0, −45, 0 s] in chord |
| TE pre-shape droop ($p_3$) | 95 mm |
| Reinforcement 1 ($d_1$) | 312 mm |
| Reinforcement 2 ($d_2/d_3$) | 370 mm/590 mm |
| Max. backward SCB crest pos./height | 586 mm/20.7 mm ($F_c$ ~ 0 N) |
| Max. forward SCB Crest pos./height | 354 mm/25.4 mm ($\varepsilon_{max}$ ~ 0.3%) |
| Max. backward position (actuator stroke 1/2) | 4.6 mm/0 mm |
| Max. forward position (actuator stroke 1/2) | 8.5 mm/− 9.5 mm |
| Airbrake (actuator stroke 1/2) | 45 mm/8 mm |

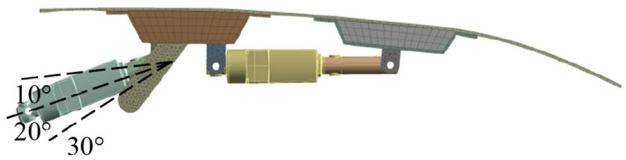


**Fig. 11** Configuration for the maximum backward position with foam core in the leading and trailing edge reinforcement and definition of the actuation angle

match the cruise target shape, the structure must be stiffened by extra plies or a honeycomb or foam core as depicted in Fig. 11 to support the structure against the aerodynamic loads. This leads to a plateau in the bump shape in intermediate bump positions between the extremal forward and backward bump crest positions (see Fig. 12). Although the bump height is reduced in these transitional shapes, this could be controlled by adapting the actuator settings.

## 2.4 Sensitivity

Since minor deviations from the desired cruise shape can easily jeopardize the benefit of the overall concept for wave drag reduction, the robustness against varying loads in cruise has to be checked. The waviness requirements, in particular, for regions in which the flow is intended to be laminar are very tight. For the position-adaptive shock control bump, therefore, the cruise shape for a variation of the assumed cruise pressure load of ± 10% is assessed.

As reference, the cruise shape of the presented "maximum backward" configuration with parameters in Table 3 is used. As given in Fig. 13, the impact of the varying pressure on the shape is very small (±0.2 mm) and located in the trailing edge part of the spoiler. This is expected since the primary actuator is attached to the front spar and to the spoiler at about $y = 160$ mm so that between these positions, there is enough stiffness to

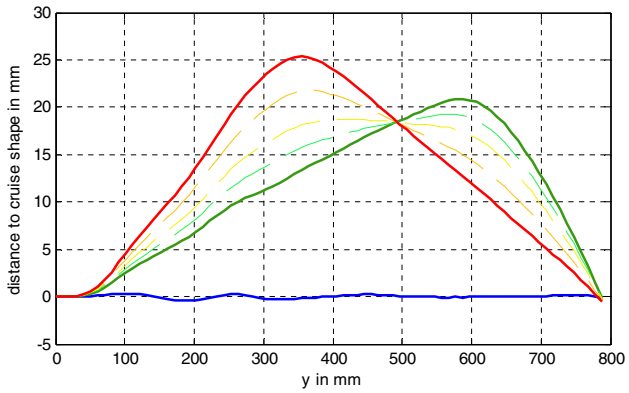


**Fig. 12** Maximum forward and backward position SCB with a max. bump height of $h_b$ = ~0.8% (26.5 mm) for $d_3$ = 590 mm and intermediate bump shapes

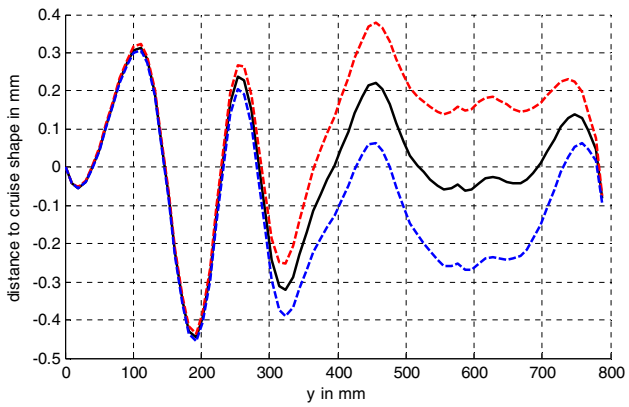


**Fig. 13** Impact of varying cruise loads (± 10%) on the cruise shape of the pre-shaped structure (black solid: cruise reference, red dashed: + 10%, blue dashed: − 10%)

transfer the aerodynamic forces to the front spar. This may be different for larger spoilers at the wings inboard position. In the following, the impact of the actuator installation of the primary actuator is investigated to identify the impact of the attachment position on the actuator forces. This knowledge is crucial since the forces are sizing the actuator and there is only limited space available especially at outboard wing position. For this reason, the actuator is placed under 10°, 20° (reference) and 30° (with constant actuator length) as given in Fig. 11. The operational parameters of the actuators (i.e., stroke) in Table 3 are adapted in a way that the bump shapes given in Fig. 12 remain the same. As expected, the rapid descent with deployed airbrake is the sizing load case for the primary actuator. Furthermore, the installation situation of the first actuator does not influence the loads on the second actuator in the assessed domain.

While the first actuator has low tension loading for the load cases 'Cruise Shape', 'Maximum Backward Bump' and 'Maximum Forward Bump', it is subjected to significantly higher compression loads in the 'Airbrake' load case. As given in Fig. 14, the maximum load depends strongly on the installation situation of the actuator. Even though higher installation angles result in reduced actuation forces, it has to be considered that the design space is small and higher installation angles will probably lead to conflicts with other system components such as actuators and sensors for the aileron and power supply at outboard wing positions.

The maximum forces on the second actuator for the forward bump deployment are comparably low. These forces can be reduced by a larger distance to the spoiler skin ($h_1$ and $h_2$) as well as by a tapered skin thickness in the forward bump hinge ($t_{b1}$). However, the minimum skin thickness for this hinge is defined by the length of the hinge since the aerodynamic loads will cause an undesired deformation if the skin gets too thin.

## 3 Full-scale structural design

To assess the deformation and actuator forces on the full-scale spoiler, the simulation is extended to a spoiler with a span of 1600 mm and a surface of approximately $A = 1.2\ m^2$. This corresponds to the size of a spoiler on commercial airplanes like, e.g., an A320.

In the full-scale model, the design of the actuator attachment points becomes more important. To achieve a 2D shape of the bump over the spoiler span and to guarantee the cruise shape of the spoiler, the design of the load introduction brackets and the substructure have been adapted for a better distribution of the loads to avoid undesired deformation or stress peaks. However, the analysis of the deformation of the spoiler panel indicates only minor deviations from the desired optimal cruise shape geometry. The typical lift-up problem of the spoiler trailing edge corners as for conventional spoilers is avoided by the pre-shaping of the spoilers trailing edge. So, the trailing edge is pre-stressed by the contact to the flap under cruise loading and, therefore, has additional stiffness that helps to generate the desired cruise shape.

For the assumed 40° airbrake functionality and the predefined actuation parameters for forming the bump at extremal positions, the required actuator forces are given below. The sizing and maximum compression actuator force is found to be the first actuator in the airbrake position with about 40 kN. Compared to existing spoiler actuators, this is not critical and in the same magnitude of maximum force for deployment. The maximum required force for airbrake deployment for the second actuator is found to be half of this value with about 20 kN. The maximum actuator forces for the holding the SCB positions or retracting is calculated in the range of 25–27 kN for both actuators (Fig. 15).

This is more challenging since the second actuator is in a position where only limited space is available. However, this issue could be solved by a 'locked' position of the actuator for compression loading since it is generally used for the deployment of the forward SCB position in tension mode.

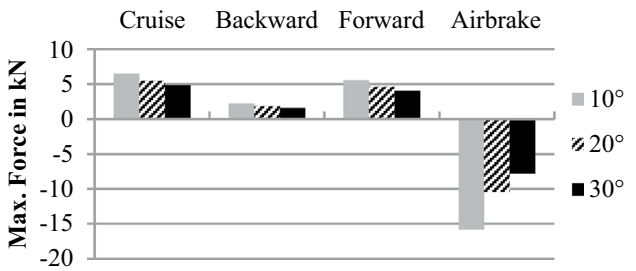


**Fig. 14** Impact of the installation angle of the primary actuator on the actuator forces

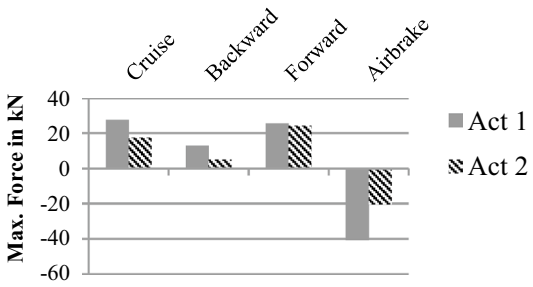


**Fig. 15** Actuator forces for the 3D − 1600 mm span position adaptive spoiler with SCB functionality

Finally, the structural strength is assessed for the full spoiler configuration with special attention given to the two hinges of the flexible hinge to the front spar and the bump hinge which forms the forward position of the SCB. As given in Fig. 16, the maximum principle strain can be found for the airbrake load case in the flexible hinge to the front spar with about $\varepsilon_1 = 0.8\%$. This is assumed as a challenge especially under the perspective of fatigue loading of the hinge and environmental impact on the structural strength. Furthermore, a double-curved state of stress as there will be for an appropriate wing bending load case is not considered in this study.

However, the maximum strain in the hinge can be further reduced using the two parameters of skin thickness and the length of the hinge. Since the skin thickness is reduced here already to a minimum (1.5 mm), a modification of the hinge length is preferable; however, this will influence the position of the attachment of the first actuator since the reinforcement for the actuator attachment bracket is shifted more backwards to the spoiler trailing edge.

## 4 Experimental validation

To validate the structural design and analysis, a functional demonstrator is developed. The 2D demonstrator is limited to a 200 mm span section with 800 mm in chord direction and design parameters as given in Sect. 2.1 (Fig. 17).

The demonstrator is manufactured from HexPly M21 prepreg material and Rohacel foam core. The guidings and fittings are made from aluminum. For laboratory purposes, the skin thickness is reduced and stacking sequence is adapted to reduce actuator forces. Main objective for the experimental validation is the correlation of deformation for the maximum forward and backward bump position to identify and assess the plateau for intermediate position between max. forward and backward position. The measurements have been performed using the optical GOM ATOS scanning system [16].

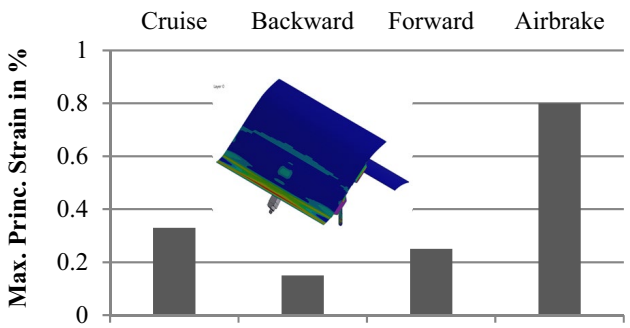


**Fig. 16** Actuator forces for the 3D – 1600 mm span position adaptive spoiler with SCB functionality

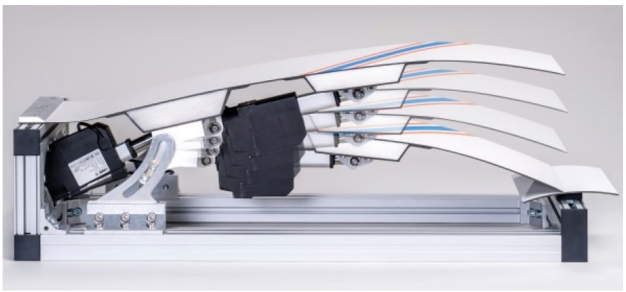

**Fig. 17** Movement overlay of functional demonstrator for validation of the structural design and analysis

In Fig. 18, the experimental SCB shapes are given. The extreme positions in chord of backward as well as forward shape are achieved as predicted in the test. However, the maximum bump height of the backward bump could not be achieved. Analyzing the forward SCB shape and comparing it with Fig. 12, it is obvious that the achieved shape in the experiment is not the predicted final shape but an intermediate shape.

It is expected that the reason for the deviation from the prediction is a misalignment of the support of the spoiler trailing edge.

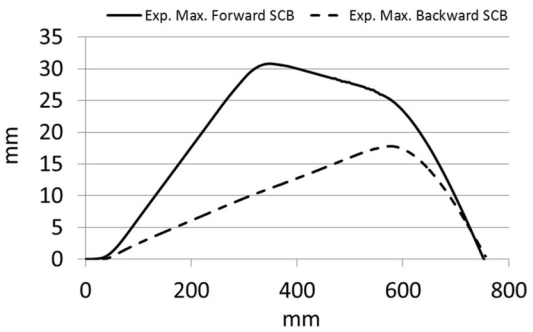


**Fig. 18** Experimental results of surface bump shape for max. backward and max. forward SCB

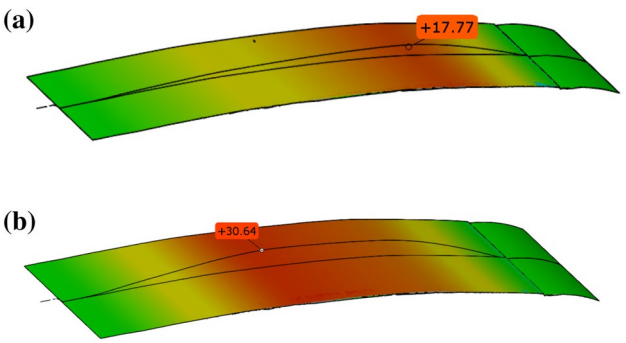


**Fig. 19** Experimental results of surface bump shape for **a** max. backward SCB and **b** max. forward SCB

In the end, Figs. 18 and 19 indicate a good, smooth shape of the rising edge of the bump and an exact positioning of the bump crest.

Further work will focus on the investigation of the impact of the plateau on the aerodynamic performance and on structural concepts to reduce the plateau if there is a major impact on the aerodynamic performance. Furthermore, the replacement of the second actuator by a mechanism is important to reduce the complexity and weight of the technology.

## 5 Summary

A concept for an adaptive spoiler shock control bump is presented. The design is based on a shock control bump spoiler concept with a pre-shaped spoiler body with fixed bump position presented by Kirn and Machunze. With the introduction of a second actuator, a forward and a backward bump position can be realized. Depending on the structural design of the reinforcing structural elements, these extremal positions can be easily adapted to the aerodynamic needs. However, the design is limited by maximum strain limitations of the material especially to the flexible-hinge design to enable laminar flow on the spoiler. Furthermore, the design space which is needed for a proper design of the brackets for the actuator attachment for load introduction and transfer is limited. Since the structural design of the spoiler does not incorporate additional structural elements or new materials, the spoilers specific weight does not change significantly. The additional functionality of a position adaptive shock control bump is, therefore, bought through the weight and complexity of a second actuator. Especially for high aspect ratio low sweep wings with slim profiles, the integration of such a new device is a challenge due to the limited available space. Here, further work has to find a solution, e.g., to replace the additional actuator by a feasible mechanism which could be coupled to the standard spoiler actuator.

**Acknowledgements** The author would like to thank S. Bauss, W. Machunze and J. Kirn from Airbus for the good collaboration and teamwork. The herepresented work has received funding by the federal ministry for economic affairs and energy within the framework of the federal aviation research programme, FkZ: 20A1302B.

**Funding** Open Access funding enabled and organized by Projekt DEAL.



## Reference

1. Schlipf, B.: Insect shielding Krüger—structural design for a laminar flow wing. In: DGLR Congress 2011, Bremen, pp. 55–60 (2011)
2. Kintscher, M., Kirn, J., Monner, H.P.: Ground testof an enhanced adaptive droop nose device. In: European Congress on Computational Methods in Applied Sciences and Engineering, ECCOMAS 2016. ECCOMAS2016—VII European Congress on Computational Methods in Applied Sciences and Engineering, 5–10 June 2016, Crete Island, Greece
3. Kintscher, M., Monner, H.P., Kühn, T., Wild, J., Wiedemann, M.: Low speed wind tunnel test of a morphing leading edge. In: AIDAA—Italian Association of Aeronautics and Astronautics XXII Conference, 09–12 Sept. 2013. Neapel, Italien
4. Fischer, M.: Stepless and sustainable research for the aircraft of tomorrow—from AFloNext to Clean Sky 2. In: 1st AFloNext Workshop Key Note Lecture No. 1, Delft, The Netherlands, 10 Sept 2015
5. Kintscher, M., Monner, H.: Structural concept of an adaptive shock control bump spoiler. SAE Tech. Paper. (2017). https://doi.org/10.4271/2017-01-2164
6. Reckzeh, D.: Multifunctional wing moveables: design of the A350XWB and the way to future concepts. In: 29th Congress of the International Council of the Aeronautical Sciences. September 7–12, St. Petersburg, Russia (2014)
7. Ashill, P.R., Fulker, J.L., Shires, J.L.: A novel technique for controlling shock strength of laminar-flow airofoil sections. In: The 1st European Forum on Laminar Flow Technology, Hamburg, pp .175–183 (1992)
8. Bruce, P.J.K., Colliss, S.P.: Review of research into shock control bumps. Shock Waves. **25**, 451–471 (2015). https://doi.org/10.1007/s00193-014-0533-4
9. Sommerer, A., Lutz, T., Wagner, S. Numerical optimisation of adaptive transonic aerofoils with variable camber. In: Proceedings of the 22nd ICAS Congress, Harrogate, UK, 27 Aug–1 Sept 2000
10. Kirn, J., Machunze, W., Weber, M., Strachauer, F.: Non-discrete spoiler with an adaptive shock control bump. In: ICAST 2016, October 3–5, 2016, Lake George, New York, USA
11. Bein, T., Hanselka, H., Breitbach, E.: An adaptive spoiler to control the transonic shock. Smart. Mater. Struct. **9**, 141 (2000) https://doi.org/10.1088/0964-1726/9/2/303
12. Campanile, L.F., Keimer, R., Breitbach, E.: The fish-mouth actuator: design issues and test results. J. Intell. Mater. Syst. Struct. **15**, 711–719 (2004). https://doi.org/10.1177/1045389X04044452
13. Wadehn, W., Sommerer, A., Lutz, T., Fokin, D., Pritschow, G., Wagner, S.: Structural concepts and aerodynamic design of shock control bumps. In: Proceedings of the 23rd ICAS Congress, Toronto, Canada, 8–13 September 2002
14. Kintscher, M., de Sousa, N.A., Monner, H.P., Wiedemann, M.: Generation of a shock control bump by pressurized chambers. In: 26th International Conference on Adaptive Structures and Technologies, 14–16 October 2015. Kobe, Japan
15. Machunze, W., Kirn, J., Weber, M.: Integral CFRP spoiler with shock bump control. In: ICCS19, 5–8 September, Porto, Portugal
16. ATOS—Industrial 3D Scanning Technology. https://www.gom.com/metrology-systems/atos.html. Accessed 10 Jan 2019.